

Interfacial Structure of Immobilized Antibodies and Perdeuterated HSA in Model Pregnancy Tests Measured with Neutron Reflectivity

Benjamin J. Cowsill,[†] Xiubo Zhao,[‡] Thomas A. Waigh,[†] Saji Eapen,[§] Robert Davies,[§] Valerie Laux,^{||} Michael Haertlein,^{||} V. Trevor Forsyth,^{||,⊥} and Jian R. Lu^{*,†}

[†]Biological Physics Group, School of Physics and Astronomy, The University of Manchester, Schuster Building, Manchester M13 9PL, U.K.

[‡]Department of Chemical and Biological Engineering, The University of Sheffield, Mappin Street, Sheffield S1 3JD, U.K.

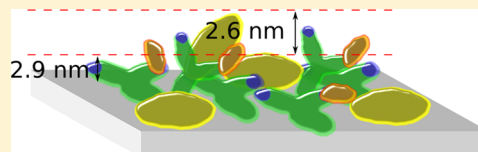
[§]SPD Development Company Ltd., Priory Business Park, Bedford MK44 3UP, U.K.

^{||}Institut Laue Langevin, 6 rue Jules Horowitz, 38042 Grenoble, France

[⊥]EPSAM/ISTM, Keele University, Staffordshire ST5 5BG, U.K.

Supporting Information

ABSTRACT: Experimental studies of antibody adsorption and antigen binding that mimicked pregnancy test immunoassays have been performed using neutron reflectivity studies of a model antibody/antigen system immobilized on the silica/water interface. The study revealed the nature of the antibody/antigen interaction and also the importance of a blocking protein, in this case human serum albumin (HSA), that enhances the immunoassay's specificity and efficiency. Of central importance to this study has been the use of a perdeuterated human serum albumin (d-HSA), providing contrast that highlights the orientation and position of the blocking agent within the adsorbed layer. It was found that the adsorbed HSA filled the gaps between the preadsorbed antibodies on the substrate, with decreased adsorption occurring as a function of increased antibody surface coverage. In addition, the antigen binding capacity of the adsorbed antibodies was investigated as a function of antibody surface coverage. The amount of specifically bound antigen was found to saturate at approximately 0.17 mg/m² and became independent of the antibody surface coverage. The ratio of bound antigen to immobilized antibody decreased with increased antibody surface coverage. These results are of importance for a full understanding of immunoassay systems that are widely used in clinical tests and in the detection of environmental contaminants.



INTRODUCTION

Immunoassays utilize the specific binding of an antibody to its antigen to measure the concentration of antigens in a test solution. They have been successfully used for over 30 years for the detection of viruses, illegal drugs, and trace contaminants^{1,2} and to quantify low levels of clinically important molecules.³ The antibodies are immobilized onto a solid substrate for most of these applications. However, the antigen binding efficiency of a surface-immobilized antibody is far lower than it is for an antibody in free solution. In order to produce more sensitive immunoassays, it is essential to understand the interfacial behavior of immobilized antibodies.

One of the most familiar immunoassays is the home use pregnancy test, an implementation of a lateral flow immunochromatographic test. This uses two monoclonal antibodies, anti- α -hCG and anti- β -hCG, that bind to the α and β epitopes of the human chorionic gonadotropin (hCG) antigen, a small protein (ca. 38 000 Da) whose presence in urine above about 25 mIU/mL (75 pM) indicates pregnancy. The anti- β -hCG antibody is immobilized as a line (ca. 1 mm wide) on a white, porous nitrocellulose membrane (labeled as the test line in Figure 1) while the anti- α -hCG antibodies are bound to colored particulates, typically a 40 nm diameter gold sol (red) or a 400 nm diameter blue latex, and held in a pad in a

dry state and mobilized by the urine onto the membrane. hCG in the test urine binds to the anti- α -hCG antibody on the particles, and capillary action causes them to pass over the test line. Here, β -hCG epitopes projecting from the particle surface can cause it to be captured by the immobilized antibody. This type of immunoassay is known as a “sandwich” format because the analyte cross-links the two antibodies just as jam sticks two slices of bread together in a sandwich.

Although there are many ways to immobilize antibodies on to a substrate,^{4,5} the least complex, cheapest, and most controllable is by physical adsorption. Antibodies are Y-shaped molecules with approximate crystalline dimensions 142 × 85 × 38 Å.⁶ Each has two antigen binding fragments (Fab) that are connected by a crystallizable fragment (Fc). One antigen may bind to each Fab, which means that each antibody has a maximum antigen binding capacity (AgBC) of 2.⁷ However, immobilized antibodies displayed AgBCs that are dramatically lower than 2.⁸ It is thought that the surface packing density and unfavorable orientations of the adsorbed antibodies restrict access of the antigen molecules to the Fabs.⁹

Received: February 28, 2014

Revised: April 28, 2014

Published: May 1, 2014

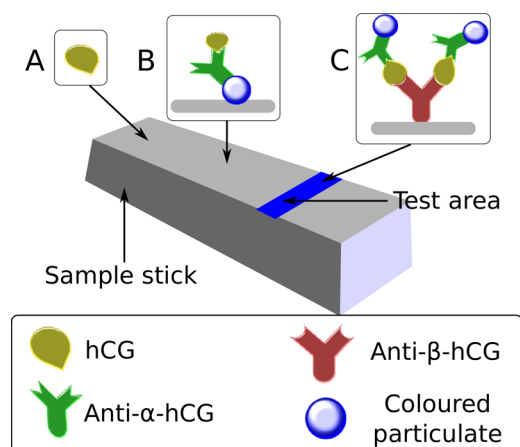


Figure 1. Schematic diagram of a lateral flow pregnancy test. Urine stream wets the left end of the sample stick, moves onto the conjugate pad containing antibody-coated colored particulate labels and further onto the test and control lines within the test area, and finally to the absorbent sink pad on the right end. During the test process hCG in the urine (A) first binds to the anti- α -hCG (B) preimmobilized on the colored particles. The capillary action of the sample stick forces the hCG/anti- α -hCG/colored particulate complex to the test area where the β epitope of the hCG binds to the immobilized anti- β -hCG antibody (C). This specific binding event anchors the particles to the test line, whose color intensity increases with the concentration of hCG. The control line will immunologically capture the label regardless of the presence of hCG to indicate that the device has worked properly and that the urine has flowed past the test line.

Pregnancy tests and other “sandwich” immunoassays are adversely affected by nonspecific adsorption: false positive results can occur if the colored particulates adsorb to the test surface in the absence of analyte. A major cause of this is the binding of the antibody on the particle to protein-free areas on the test line. Protein blocking agents, such as serum albumin and β -casein and detergents, such as Tween 20, are commonly employed to counteract this. However, few studies have investigated the molecular arrangement of coadsorbed blocking agents. It is unknown whether the blocking agent slots between or settles on top of the preadsorbed antibodies or how effective they are at filling in the antibody free areas on the two surfaces (test line and particle).

Here we use neutron reflection (NR) to investigate the structural arrangement of the proteins on a model pregnancy test surface. NR is one of the few techniques that are able to accurately determine the surface coverage, density, and thickness of adsorbed antibodies.¹⁰ The model surface was built up in stages so that the molecular structure of the adsorbed film could be determined. Perdeuterated human serum albumin (d-HSA) was used to highlight the blocking agent, human serum albumin (HSA), so that its orientation and position within the adsorbed antibody layer could be accurately determined. Deuterated HSA was also used in this study to enhance the contrast between d-HSA, H_2O , and the antibody/antigen, thereby allowing a more detailed understanding of the HSA–antibody interaction.

NEUTRON REFLECTION

The theory behind specular NR has been described elsewhere.^{11–13} Neutrons are reflected by interfaces in a similar way to light,¹⁴ and due to the small wavelength of neutrons (1–10 Å), NR can measure the thickness of thin films with a sensitivity

of 2–3 Å. Although X-ray reflectivity is also able to achieve this sensitivity, NR does not damage the sample and can be used to perform *in situ* experiments.

NR measurements are affected by the scattering length and other physical constants that vary between isotopes. In particular, the scattering length density (SLD) of a surface varies with its chemical composition such that

$$\rho = \sum b_i n_i \quad (1)$$

where ρ is the SLD and n_i and b_i are the respective number density and the scattering length of element i . D_2O ($\rho = 6.35 \times 10^{-6} \text{ Å}^{-2}$) is typically used as a solvent for NR experiments. Since the SLD of D_2O is different to silicon oxide ($3.41 \times 10^{-6} \text{ Å}^{-2}$) and hydrogenated HSA ($3.33 \times 10^{-6} \text{ Å}^{-2}$ for h-HSA), good contrast is achieved between the different surface layers. Meanwhile, H_2O has an SLD of $-0.56 \times 10^{-6} \text{ Å}^{-2}$.

Although H_2O and D_2O are chemically similar, the difference between their SLDs is large and can be exploited by NR experiments. In this study, we have used NR to investigate the adsorption of mixed antibody/HSA layers, and the use of hydrogenated and deuterated species of HSA in both D_2O and H_2O allowed the antibody and HSA components to be highlighted separately. The deuterated HSA (d-HSA) had a larger SLD ($7.9 \times 10^{-6} \text{ Å}^{-2}$ in D_2O and $6.4 \times 10^{-6} \text{ Å}^{-2}$ in H_2O) than hydrogenated HSA. Therefore, when h-HSA was adsorbed to silica from D_2O , the majority of the reflectivity signal was due to the adsorbed antibody, owing to the larger contrast between the SLD of the antibody and D_2O . The large contrast between the SLDs of d-HSA and H_2O enhanced neutron scattering of the d-HSA over that of the preadsorbed antibody, enabling it to be characterized within the mixed protein layer in H_2O .

The reflectivity, R , is defined as the ratio of reflected to incoming neutron intensity. R varies with the momentum transfer, q , perpendicular to the interface and is given by

$$R(q) = \frac{16\pi^2}{q^2} |\rho(q)|^2 \quad (2)$$

where q is given by eq 3

$$q = \frac{4\pi}{\lambda} \sin \theta \quad (3)$$

and θ is the incident angle of the neutron beam.

Adsorbed films typically contain solvent (D_2O or H_2O) in addition to protein. The following equation can be used to calculate the protein volume fraction, ϕ_p , of a mixed protein/solution film:

$$\phi_p = \frac{\rho_f - \rho_s}{\rho_p - \rho_s} \quad (4)$$

where ρ_f , ρ_s , and ρ_p are defined as the SLDs of the film, pure solvent, and pure protein, respectively.

Optical matrix formalism¹⁵ is often used for the analysis of reflectivity profiles. In a typical NR data analysis routine, the measured reflectivity data are compared to calculated reflectivity profiles. The calculated profiles are based on any number of uniform layers that each have a unique SLD and thickness, τ . The chosen model should fit the measured data as closely as possible but have a minimum number of fitted layers. Only when samples have nonuniform SLD distributions should multiple layers be added to the model.

In these types of experiment, it is possible that more than one model may fit the experimental data. In these instances parallel NR experiments can be performed in D₂O and H₂O to determine which model more correctly describes the measured data, as there will be fewer models that can fit the data from both solvents. These studies together with the use of d- and h-proteins help narrow down the possible models further. In some cases, the model fits well to the measured data mathematically but makes little sense physically and so this can be used to exclude some models.

The average area occupied by a protein, a , can be calculated from

$$a = \frac{V_p}{\tau\phi_p} \quad (5)$$

where V_p is the volume of the protein. The surface mass coverage, M , can then be calculated from a :

$$M = \frac{M_w}{N_A a} \quad (6)$$

where N_A is Avogadro's number and M_w is the molecular weight of the protein.

For a protein that is coadsorbed onto a preadsorbed layer, eq 7 can be used to calculate the volume fraction of the coadsorbed protein, ϕ_y :

$$\phi_y = \frac{\rho_{l(x+y)} - \rho_{lx}}{\rho_y - \rho_s} \quad (7)$$

where $\rho_{l(x+y)}$ is the SLD of the mixed protein layer and ρ_{lx} is the SLD of the preadsorbed layer.

EXPERIMENTAL METHODS

Materials. Perdeuterated human serum albumin (d-HSA) was expressed as secreted protein in *Pichia pastoris* GS115 (Invitrogen), with details of the isotope labeling procedure described elsewhere.¹⁶ d-HSA was purified from the *P. pastoris* supernatant by ammonium sulfate precipitation and fatty acid removal by Lipidex 1000 treatment.¹⁷ d-HSA was used as a blocking agent instead of conventional, hydrogenated HSA in one experiment.

Purified monoclonal antibodies (anti- α -hCG, clone 3299, anti- β -hCG, clone 3468) and the antigen human chorionic gonadotropin (hCG) purified from human urine (SciPacLtd UK, Product Code: P111-0) were kindly supplied by SPD Development Company Ltd. as stock solutions in phosphate buffered saline (PBS), 0.1% sodium azide, pH 7.4, and were diluted to the required concentrations using the PBS buffer prepared at pH 5 by using the appropriate ratios of Na₂HPO₄, NaH₂PO₄, and H₃PO₄ to give the total ionic strength of 20 mM. The final solution pHs were checked, and any minor pH differences were then adjusted with concentrated HCl or NaOH. All albumin solutions were prepared in the same PBS buffer. The molecular weights of the antibodies were close to 150 000 Da, and their isoelectric points were 5.5–6.0; the molecular weight of hCG was 38 000 Da, and its isoelectric point was around 5.5. Neutron measurements were made in either D₂O or H₂O in order to highlight the interfacial isotopic contrasts involving h-HSA, d-HSA, and the other proteins.

Neutron Reflection Liquid Cell Setup and Model Assay Test Procedures. One of the large surfaces of a (111) silicon block (with approximate dimensions of 1.2 × 4.0 × 6.0 cm³) was polished by Crystran Ltd., Poole, UK. The block was immersed in a piranha solution (in a volume ratio of 6:1 for H₂SO₄ (98%) to H₂O₂ (35%)) at about 90 °C for 1 min to maximize its surface hydrophilicity. It was then taken out, cooled down, and washed with plenty of distilled water before it was placed in a 5% (w/w) solution of Decon 90 (Decon Ltd., Hove, UK) for 5 min. The Decon washed surface was subsequently

rinsed with a large amount of ultrahigh quality water (UHQ). The cleaning process formed a reproducible silicon oxide layer of thickness 12 ± 3 Å on the polished surface of the block, as measured by a UVISEL ellipsometer (Horiba Jobin Yvon, Stanmore, UK). The same Decon washing was used to remove adsorbed proteins and regenerate the silicon oxide surface between subsequent protein adsorption measurements. The reproducible surface properties were confirmed by identical lysozyme adsorption at 1 mg/mL, pH 7.^{9,10} A Perspex trough with attached flow system was clamped against the cleaned surface of the block. Protein and buffer solutions were introduced to the block surface via the trough's flow system.

The immunoassay was constructed in stages. First, antibody to the α -hCG subunit was introduced to the cleaned silicon surface and allowed to adsorb for 1 h before reversibly adsorbed molecules were washed from the surface with phosphate buffer, care being taken not to allow air to contact the surface of the block. The block was then placed on the NR beamline, and reflectivity data were recorded as a function of wave vector transfer. Each NR measurement typically took 1 h (including sample changer time). The reflectivity was measured first in D₂O and then in H₂O, using an HPLC pump to exchange solvents.

After the antibody measurement, 25 µg/mL of h-HSA was adsorbed for about 1 h and subsequently rinsed before the reflectivity was measured in both D₂O and H₂O. Finally, 2.0 µg/mL of hCG was introduced to the surface of the block and washed after an adsorption time of 1 h. This hCG concentration corresponds to about 9250 mIU/mL, or 27.7 nM, which is about 30× the equilibrium binding constant for this antibody. Theoretically, and in practice, this means that any available (exposed) binding sites of the antibody would be occupied by hCG under these conditions. Reflectivity profiles were used to determine the thickness and scattering length density of each adsorbed sample. Samples and buffers were introduced to the block with either a syringe or an HPLC pump.

The model immunoassay was constructed at high, medium, and low antibody surface coverages. Different adsorption times were used to vary the antibody surface coverage: longer adsorption times resulted in higher surface coverages.

Neutron Reflection Measurements. Neutron reflectivity measurements were made on the SURF reflectometer at the ISIS pulsed neutron source near Oxford, UK. Measurements were made using a single detector at fixed angles (θ) of 0.5°, 0.8°, and 1.8° and for neutron wavelengths (λ) in the range 0.5–6 Å to provide a momentum transfer range of 0.012–0.5 Å^{−1}. The absolute reflectivity was calibrated with respect to the 100% reflectivity below the critical edge of D₂O, and the background was determined from the reflectivity at the limit of high q (>0.25 Å^{−1}). Similar reflectivity measurements were also made at the D17 reflectometer at the Institut Laue-Langevin, Grenoble, France. Measured reflectivity profiles were analyzed using our own software developed from optical matrix formulas.⁹ Where parallel measurements were made under different isotopic contrasts, care was taken to obtain the most consistent structural parameters through optimizing the fitting quality via visual assessment and χ^2 values (measuring deviations between measured and calculated data).

RESULTS AND DISCUSSION

Parallel NR experiments with solvents and proteins of different scattering length densities, making full use of isotopic replacement, add greatly to the "imaging power" of this technique. This reduces both the number of theoretical models that fit the data and the ambiguity in the inferred interfacial structure. Furthermore the ability to use macromolecular deuteration in this way allows specific components to be distinguished from other interfacial materials. This approach was particularly useful for multiple component systems, such as the model immunoassay described here.

Characterization of Perdeuterated HSA. Since the interfacial adsorption of d-HSA onto a bare SiO₂ surface has not been studied, it was of interest to establish if its behavior was similar to h-HSA. Figure 2 shows the neutron reflectivity

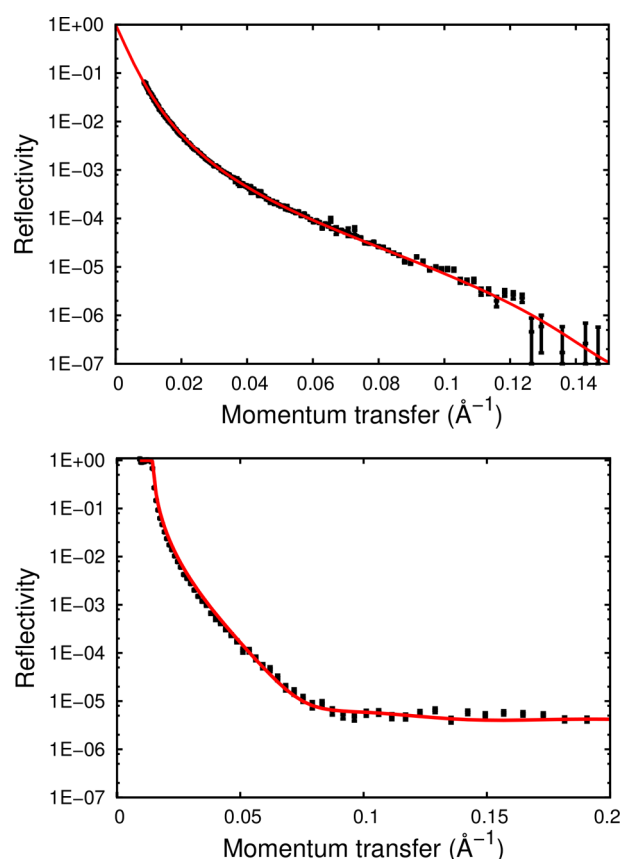


Figure 2. Reflectivity profiles for 25 $\mu\text{g/mL}$ d-HSA adsorbed at the $\text{SiO}_2/\text{H}_2\text{O}$ interface (top) and 25 $\mu\text{g/mL}$ h-HSA adsorbed at the $\text{SiO}_2/\text{D}_2\text{O}$ interface (bottom). Both samples were made in 20 mM phosphate buffer, pH 5. For each sample, the red line represents the best fitting uniform layer model with parameters as listed in Table 1.

from a typical adsorption from 25 $\mu\text{g/mL}$ of d-HSA. The parameters obtained from the best fit (red line in Figure 2) are listed in Table 1 along with the corresponding values for 25 $\mu\text{g/mL}$ h-HSA measured with NR at the $\text{D}_2\text{O}/\text{SiO}_2$ interface.

Table 1. Parameters Extracted from Uniform Layer Model Fits to the NR Data Using the Optical Matrix Method^a

sample	thickness (nm)	surface coverage (mg/m^2)	volume fraction	area per molecule (nm^2)
h-HSA	3.4 ± 0.5	1.6 ± 0.5	0.34 ± 0.05	72 ± 10
d-HSA	3.4 ± 0.5	1.6 ± 0.5	0.34 ± 0.05	72 ± 10

^aThe parameters are for 25 $\mu\text{g/mL}$ h-HSA, measured in D_2O , and 25 $\mu\text{g/mL}$ d-HSA, measured in H_2O .

A uniform layer model with similar parameters provided the best fit for both h-HSA and d-HSA adsorbed films. Both d-HSA and h-HSA formed uniform layers with thicknesses at 3.4 nm, less than the 4 nm short axis of the native HSA,^{18,19} but similar to the 3 nm derived from X-ray diffraction of the crystal structure.²⁰ In addition, the area per molecule for each sample was greater than its cross-sectional area of 44 nm^2 at pH 5.¹⁹ The exact adsorbed amount was sensitive to pH and ionic strength for a given interface. This suggested that both samples adsorbed in the flat-on position (with all three HSA domains²⁰ in contact with the substrate) and became flattened on the silica surface. At pH 5, both HSAs were close to their isoelectric points, while the surface was negatively charged.²¹ Any

flattening might reflect the weak electrostatic interaction between adsorbed molecules, which would allow the molecules to spread across the surface upon direct contact.^{22,23} The surface coverage and volume fractions were closely comparable for both samples. Overall, our results show that the main features of adsorption for d-HSA were similar to those of h-HSA. Therefore, d-HSA was deemed to be a suitable alternative for h-HSA as the blocking agent in the model immunoassay.

Immunoassay Characterization. A 10 $\mu\text{g/mL}$ antibody solution was introduced to a cleaned NR block with a SiO_2 layer of thickness 12 ± 3 Å. After equilibration for 1 h, the solution was drained and the surface was rinsed with D_2O 20 mM phosphate buffer, pH 5, before the trough was subsequently filled with D_2O . A reflectivity profile obtained from the interfacial system is shown in the top panel of Figure 3. Although a uniform-layer model (blue line) almost fits the

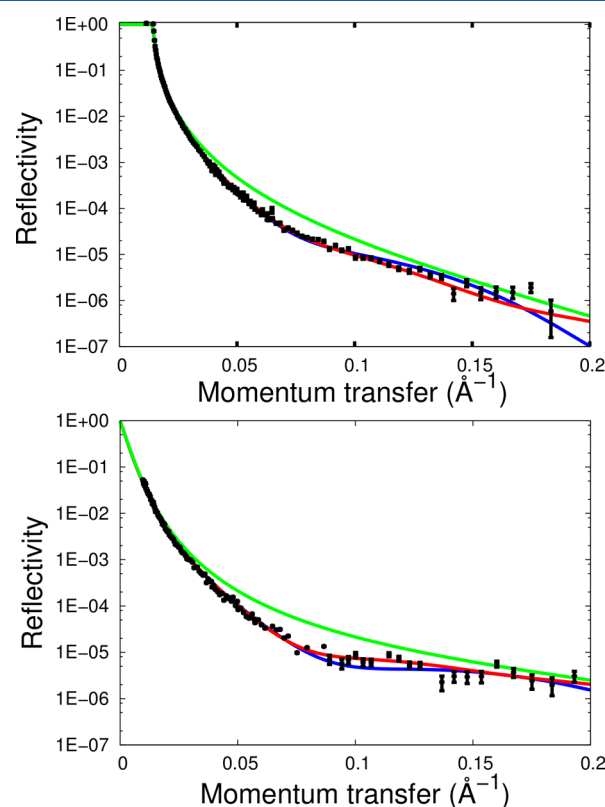


Figure 3. Top: reflectivity profile for anti- α -hCG adsorbed on to a bare SiO_2 surface as measured in D_2O buffer. The red line represents the best fitting of the two-layer model, and the blue line represents the best fitting uniform-layer model. The green line denotes the reflectivity measured at the bare SiO_2 layer/ D_2O interface. Bottom: the same anti- α -hCG measured in H_2O .

reflectivity profile, it can be seen to diverge from the experimental data at momentum transfer values greater than 0.1 \AA^{-1} . The two-layer model (red line), which consisted of an inner layer of thickness 2.8 nm and $\rho = 5.4 \times 10^{-6} \text{\AA}^{-2}$ and an outer layer of thickness 2.2 nm and $\rho = 6.0 \times 10^{-6} \text{\AA}^{-2}$, provided a closer fit to the experimental data.

A parallel reflectivity curve was obtained in H_2O in order to reduce the ambiguity of the fitted models. The bottom panel of Figure 3 shows the reflectivity profile for the same antibody sample as measured in H_2O . The reflectivity profile of the H_2O experimental data can be seen to deviate from the SiO_2 layer

Table 2. Parameters Extracted from NR Data Analysis for an Antibody/d-HSA/hCG Model Immunoassay Using the Best Fitting Model and the Optical Matrix Method^a

solvent	sample	layer no.	thickness, τ (nm)	SLD, ρ ($\times 10^{-6} \text{ \AA}^{-2}$)	volume fraction, φ_w $\varphi_{\text{d-HSA}}, \varphi_{\text{hCG}}$	surface coverage, M_w $M_{\text{hCG}}, M_{\text{d-HSA}}$ (mg/m ²)	total surface coverage (mg/m ²)
D ₂ O	A	1	2.8 \pm 0.4	5.40 \pm 0.05	0.315, 0, 0	1.33, 0, 0	2.13
		2	2.2 \pm 0.4	6.00 \pm 0.05	0.116, 0, 0	0.8, 0, 0	
	α , d-HSA	1	2.4 \pm 0.4	5.90 \pm 0.05	0.315, 0.325, 0	1.33, 1.06, 0	2.83
		2	2.3 \pm 0.4	6.03 \pm 0.05	0.116, 0.019, 0	0.8, 0.06, 0	
	α , d-HSA, hCG	1	2.9 \pm 0.4	5.80 \pm 0.05	0.315, 0.325, 0.034	1.33, 1.06, 0.08	3.00
		2	2.6 \pm 0.4	5.90 \pm 0.05	0.116, 0.019, 0.044	0.8, 0.06, 0.09	
H ₂ O	A	1	3.8 \pm 0.4	0.00 \pm 0.05	0.237, 0, 0	1.36, 0, 0	1.69
		2	2.0 \pm 0.4	-0.30 \pm 0.05	0.110, 0, 0	0.33, 0, 0	
	α , d-HSA	1	2.8 \pm 0.4	1.50 \pm 0.05	0.237, 0.216, 0	1.36, 0.84, 0	2.64
		2	2.7 \pm 0.4	-0.10 \pm 0.05	0.110, 0.028, 0	0.33, 0.11, 0	
	α , d-HSA, hCG	1	3.0 \pm 0.4	1.60 \pm 0.05	0.237, 0.216, 0.042	1.36, 0.84, 0.10	2.84
		2	2.5 \pm 0.4	0.02 \pm 0.05	0.110, 0.028, 0.051	0.33, 0.11, 0.10	

^a φ_w , $\varphi_{\text{d-HSA}}$, and φ_{hCG} denote respective volume fraction for antibody, HSA, and hCG. M_w , $M_{\text{d-HSA}}$, and M_{hCG} denote respective surface coverage for antibody, HSA, and hCG.

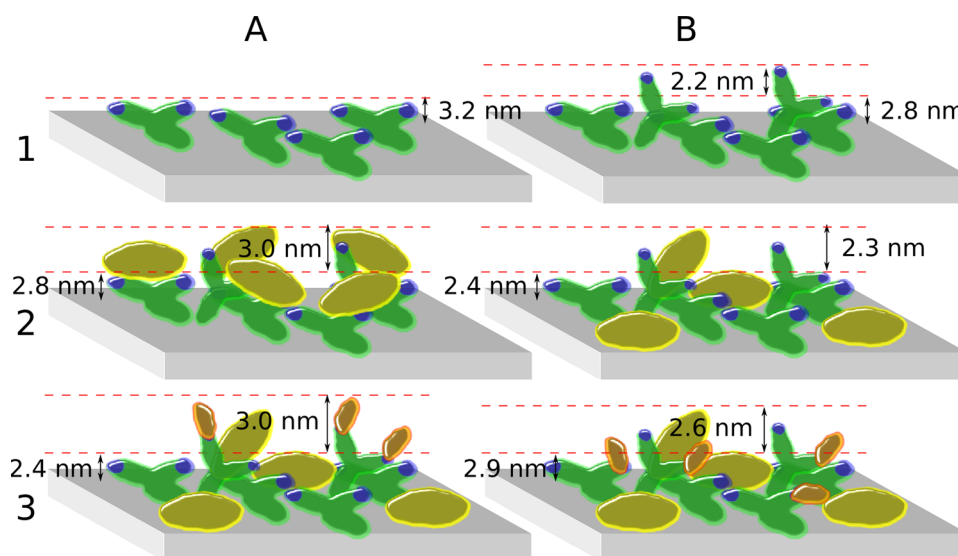


Figure 4. Antibody interfacial arrangements as revealed by NR data analysis. The green Y-shapes are the antibodies, and blue patches represent their hCG binding sites. The d-HSA molecules and hCG antigens are yellow and orange, respectively. (A1) Uniform antibody layer of 3.2 nm. (B1) The majority of the antibody molecules adsorb in the flat-on orientation to form an inner layer of 2.8 nm. Some molecules overlap the flat-on adsorbed antibodies to produce a less dense 2.2 nm outer layer. (A2) d-HSA molecules inserted into the outer antibody layer only. (B2) The d-HSA molecules slot in between the adsorbed antibody molecules. (A3) hCG molecules bind exclusively to antibody Fabs in the outer layer. (B3) hCG molecules bind to create an even distribution of hCG molecules in the inner and outer layers.

(green line), clearly indicating adsorption of the antibody as observed from the measurement in D₂O. Again, a uniform layer model (blue line) provided a reasonable fit to the experimental data but clearly did not fit the measured data in the momentum transfer range 0.1–0.15 Å⁻¹. The two-layer model (red line) better fitted the experimental data, and the parameters extracted from this were in excellent agreement with those from the D₂O run, as shown in Table 2. The two models used to fit the reflectivity curves are depicted in panels A1 and B1 of Figure 4.

The total surface coverage of the adsorbed antibody film was measured to be 2.13 mg/m² in D₂O and 1.69 mg/m² in H₂O. The two-layer models for both solvents suggested a denser inner layer (volume fraction 0.32 for D₂O and 0.24 for H₂O) and a more diffuse outer layer (volume fraction 0.12 and 0.11 for D₂O and H₂O, respectively). The antibody arrangement is schematically shown in panel B1 of Figure 4, illustrating that

most antibodies adsorbed in the flat-on orientation with some molecular overlap, forming a dense inner layer and a diffuse outer layer. The two-layer models for each solvent were used as the basis for the models of the subsequent samples.

25 μg/mL of d-HSA was then introduced to the preadsorbed antibody surface and adsorbed until equilibration before being rinsed with buffer. The reflectivity profiles for the D₂O and H₂O runs are shown in Figure 5. Two different models were examined to determine where, and in which orientation, the d-HSA was inserted into the antibody layers. The blue lines show the best fit for d-HSA inserted exclusively into the outer layer, as depicted in panel A2 of Figure 4, while the red lines are the best fit for d-HSA molecules inserted into both antibody layers, as shown in panel B2 of Figure 4. The model based on the d-HSA molecules being inserted into both antibody layers provided the closest fit to the experimental data. The best-fitting model for both solvents revealed that approximately 1

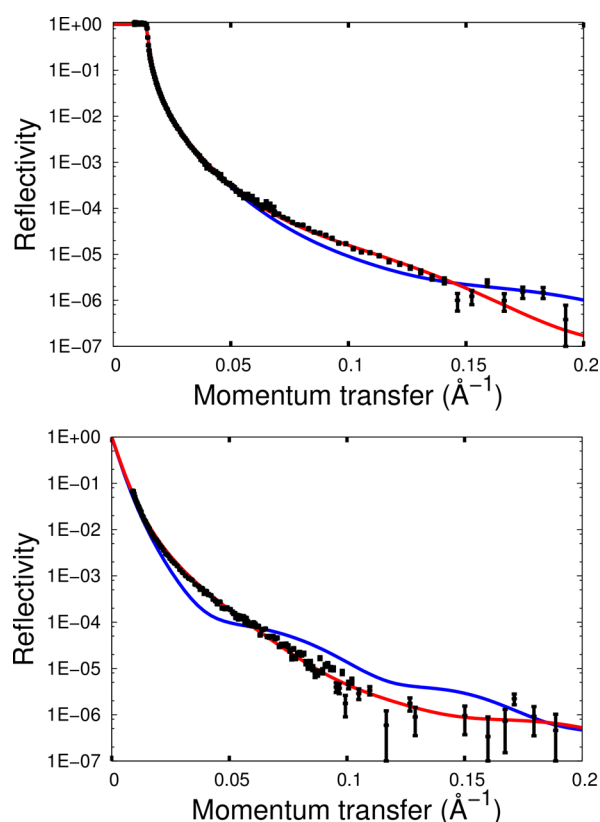


Figure 5. Top: reflectivity profile for d-HSA introduced to a preadsorbed anti- α -hCG film measured in D_2O . The red line represents the best fitting model where the d-HSA is present in both the inner and outer layers, and the blue line represents the best fitting model where d-HSA is present in the outer layer only. Bottom: the system measured in H_2O . The colored lines represent the same models as for the D_2O data.

mg/m^2 of d-HSA was inserted into the inner layer and approximately $0.1 mg/m^2$ into the outer layer. This increased the volume fraction of the inner layer by 0.33 and 0.22 for the D_2O and H_2O runs, respectively, while the volume fraction of the outer layer increased by 0.02 and 0.03, respectively, showing a large difference.

The addition of d-HSA resulted in a decrease in the thickness of the inner layer from 2.8 to 2.4 nm in D_2O and from 3.8 to 2.8 nm in H_2O . However, the combined thickness of the inner and outer layers remained approximately constant for each solvent; the D_2O run saw a decrease from 5.0 to 4.7 nm and the H_2O run a decrease from 5.8 to 5.5 nm. These thicknesses are close to the length of the 4 nm short axis of albumin;¹⁹ it would therefore appear that the d-HSA molecules also adsorb in the flat-on orientation between the flat-on adsorbed antibodies to create a thin layer of high volume fraction. Where the spaces between the antibody molecules are of insufficient size for the d-HSA molecules to adsorb, only part of the d-HSA molecule may adsorb on the surface while the rest of the molecule overlaps other d-HSA and antibody molecules to create an outer layer of low volume fraction.

It is worth noting that the addition of d-HSA to the antibody layer increased the scattering length density for the D_2O run from 5.40×10^{-6} to $5.90 \times 10^{-6} \text{ \AA}^{-2}$ for the inner layer and from 6.00×10^{-6} to $6.03 \times 10^{-6} \text{ \AA}^{-2}$ for the outer layer. Typically, for D_2O runs, an increase in the scattering length density toward the scattering length density of D_2O ($6.35 \times$

10^{-6} \AA^{-2}) would suggest that the adsorbed sample had been removed from the surface and replaced with pure D_2O . However, the scattering length density of the d-HSA was higher than D_2O and would have caused the scattering length density of the layer to increase if d-HSA was inserted into the layer. The insertion of d-HSA was confirmed by the H_2O run, which detected an increase in the scattering length density of the layer (away from the negative scattering length density of H_2O) when d-HSA was added to the antibody-coated block.

After the d-HSA measurements, $2 \mu g/mL$ of hCG was introduced and allowed to bind to the antibody surface for 1 h before buffer washing. Reflectivity profiles for the D_2O and H_2O runs are shown in Figure 6. The blue lines are for a model

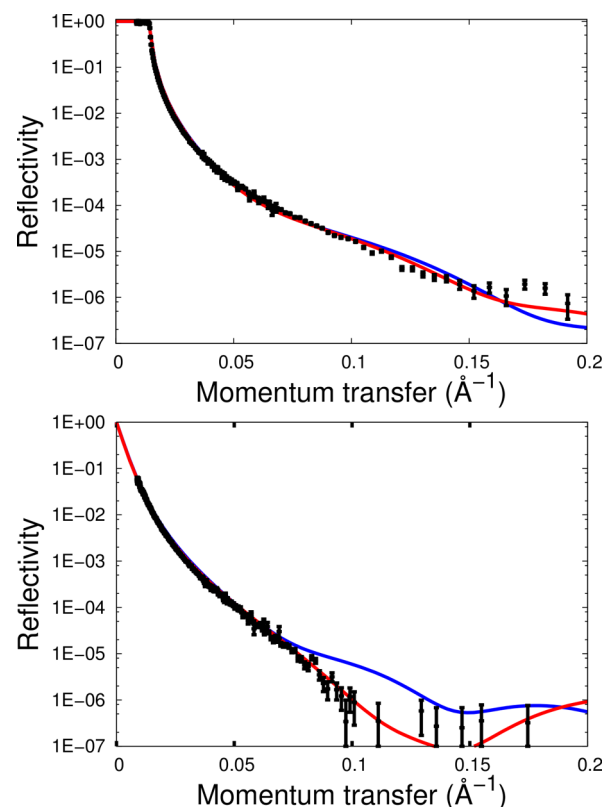


Figure 6. Top: reflectivity profile for hCG introduced to the preadsorbed anti- α -hCG/d-HSA mixed film, measured in D_2O . The red line represents the best fitting model with hCG present in both the inner and outer layers, and the blue line represents the best fitting model where the hCG is only present in the outer layer. Bottom: measurement of the same system in H_2O .

that assumes that hCG is bound exclusively to antibody Fabs in the outer layer and the red lines for a model that allows for hCG to bind to antibody Fabs in either the inner or outer layer, as shown in panels A3 and B3 of Figure 4, respectively. For both solvents the latter model, with similar parameters from both contrasts, was the only one able to adequately fit the experimental data. Thus, the best fitting model for the antibody/d-HSA/hCG system revealed that hCG was inserted into both the inner layer and the outer layer. After the introduction of hCG, the D_2O and H_2O runs both saw an increase in the surface coverage of approximately $0.2 mg/m^2$ that was evenly distributed between the inner and outer layers. This interfacial structure, in which the hCG molecules access

and bind to the antibody Fabs in both layers, is shown in panel B3 of Figure 4.

A parallel experiment was also performed, but with the d-HSA replaced by h-HSA. The results for this experiment are shown in Table S1 of the Supporting Information. The best fitting model for the antibody adsorption step was a two-layer model that had a dense inner layer of thickness 3.5 nm and SLD $5.26 \times 10^{-6} \text{ \AA}^{-2}$ and a more diffuse outer layer of thickness 2.5 nm and SLD $6.06 \times 10^{-6} \text{ \AA}^{-2}$. This antibody layer had a similar interfacial structure to the previous experiment and was used to compare the coadsorption of h-HSA (i.e., after antibody adsorption) with the coadsorption of d-HSA shown in Table 2. The coadsorbed h-HSA was found to adsorb mainly to the interface, between the antibody molecules. The d-HSA increased the surface coverage of the inner layer by 0.53 mg/m^2 but increased the surface coverage of the outer layer by only 0.08 mg/m^2 . Meanwhile, the thickness of the inner and outer layers remained roughly constant. The interfacial structure of the mixed antibody/h-HSA film was thus very similar to that of the mixed antibody/d-HSA film.

HSA Coadsorption and Antigen Binding. To determine the effects of antibody surface coverage on HSA coadsorption and antigen binding, the NR experiment was repeated at high, medium, and low antibody concentrations. Figure 7 shows how

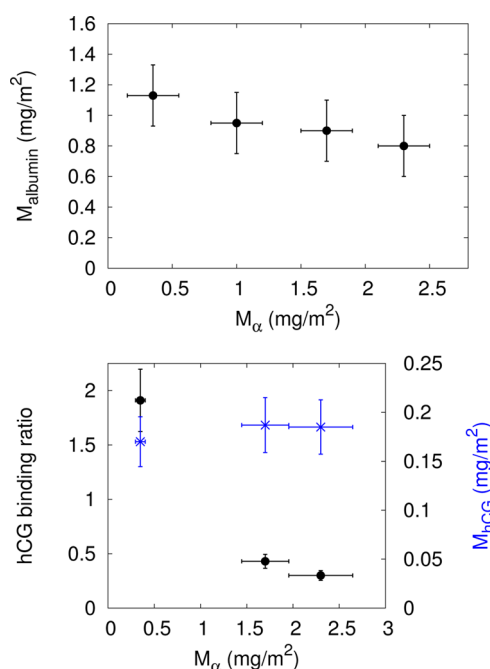


Figure 7. Top: albumin surface coverage as a function of anti- α -hCG surface coverage. The amount of albumin can be seen to decrease with increased anti- α -hCG surface coverage, which suggests that the albumin can only adsorb in the unoccupied spaces between the anti- α -hCG molecules. Bottom: hCG binding ratio (black circles, left axis) and hCG surface coverage (blue cross, right axis) as a function of anti- α -hCG surface coverage.

the surface coverage of the HSA varied with antibody surface coverage when measured by NR. The surface coverage of the HSA decreased with increased antibody surface coverage. If the albumin was coated on the antibody, as in panel A2 of Figure 4, then the albumin surface coverage would not be expected to show this trend. The reduction in albumin surface coverage at higher antibody surface coverage suggests that antibody

molecules occupied the SiO₂ surface at the expense of albumin molecules. Thus, the trend shown in Figure 7 provides further evidence that albumin largely slots into the spaces on the surface between the antibody molecules, as shown in panel B2 of Figure 4. The interfacial parameters of the low (0.35 mg/m^2) and high (2.39 mg/m^2) surface coverage antibody films are shown in the Supporting Information in Tables S2 and S3, respectively.

Figure 7 shows that the hCG adsorbed amount was largely independent of the antibody surface coverage for the NR experiments. At high, medium, and low antibody surface coverage the amount of hCG bound to the antibody Fabs remained approximately constant at 0.17 mg/m^2 ; a similar finding was also made by Zhao et al. for the hPSA antibody and its antigen,²⁴ and close to the 0.15 mg/m^2 we have previously measured with dual polarization interferometry.²⁵ However, Figure 7 also shows that the hCG binding ratio, defined as the number of bound hCG antigen molecules per antibody molecule, rapidly decreased with increased antibody surface coverage, even though the antigen was available in excess. These findings suggest that a significant number of antibody binding sites were not able to bind to the hCG at higher antibody surface coverages. This phenomenon was previously observed by Xu et al.¹⁰ for anti- β -hCG/hCG, who showed that the experimental parameter with the largest effect on the antigen binding ratio was the surface packing density of the antibody. Xu et al. also demonstrated that when antibody binding sites were in close proximity, they blocked access to the antigen.

For commercial immunoassays, these findings suggest that there is no advantage in increasing the antibody surface coverage above a certain level. Further adsorption of antibodies is unnecessary as the antibody binding sites are not accessible for the antigen to bind to and, as such, offer no increase in the sensitivity of the immunoassay. This finding is often supported by empirical work in which the amount of a particulate label bound to the test line at a fixed concentration of hCG decreases when the concentration of antibody increases above a certain level. Thus, considerable financial savings could be achieved by using only the minimum amount of (often expensive) antibodies necessary to achieve the optimum antibody surface coverage for a given substrate.

CONCLUSIONS

A simplified pregnancy immunoassay was constructed on a SiO₂ surface and investigated with NR. The thickness and density measurements obtained by NR provided evidence of d-HSA and h-HSA insertion into the gaps on the surface between the antibody molecules. In addition, the amount of adsorbed HSA was reduced when the amount of preadsorbed antibody was increased. These findings suggest that albumin adsorption provides an effective way to fill adsorption sites on the substrate and hence block the nonspecific adsorption of both hCG and the antibody on the particulate label at the surface of an immunoassay substrate. The antibody/antigen binding ratio was also investigated. It was found that the total amount of adsorbed antigen became independent of the antibody surface coverage and remained constant at approximately 0.17 mg/m^2 . However, the antibody/antigen molar binding ratio was dramatically reduced at high antibody surface coverage. This was likely to be due to the close proximity of the antibody binding sites to other adsorbed protein, rendering them inaccessible to hCG. The results imply that above a certain

antibody surface coverage there is no advantage in the adsorption of more antibody molecules, as there is no increase in the amount of bound antigen and device sensitivity.

■ ASSOCIATED CONTENT

Supporting Information

Tables S1–S3. This material is available free of charge via the Internet at <http://pubs.acs.org>.

■ AUTHOR INFORMATION

Corresponding Author

*E-mail j.lu@manchester.ac.uk; Tel +44 (0)161 3063926 (J.R.L.).

Notes

The authors declare no competing financial interest.

■ ACKNOWLEDGMENTS

We acknowledge ISIS and ILL for the provision of neutron beamtime on instruments SURF and D17 respectively. We also acknowledge the use of the Deuteration Facility as part of ILL's Life Sciences group in the Grenoble Partnership for Structural Biology (PSB). V.T.F. acknowledges support from EPSRC under Grant EP/C015452/1. The work also benefited from the JRA activities of EU Award 226507-NMI3. We thank SPD Development Company Ltd. and University of Manchester for a joint studentship for BC and EPSRC for sponsorship under Grant EP/F062966/1 for biosensor research.

■ REFERENCES

- (1) Birnbaum, S.; Uden, C.; Magnusson, C. G. M.; Nilsson, S. Latex-based thin-layer immunoaffinity chromatography for quantitation of protein analytes. *Anal. Biochem.* **1992**, *206*, 168–171.
- (2) Al-Qahtani, A.; Muttukrishna, S.; Appasamy, M.; Johns, J.; Cranfield, M.; Visser, J. A.; Themmen, A. P.; Groome, N. P. Development of a sensitive enzyme immunoassay for anti-Müllerian hormone and the evaluation of potential clinical applications in males and females. *Clin. Endocrinol.* **2005**, *63*, 267–273.
- (3) Lonnberg, M.; Drevlin, M.; Carlsson, J. Ultra-sensitive immunochromatographic assay for quantitative determination of erythropoietin. *J. Immunol. Methods* **2008**, *339*, 236–244.
- (4) Hoffman, W. L.; O'Shannessy, D. J. Site-specific immobilization of antibodies by their oligosaccharide moieties to new hydrazide derivatized solid supports. *J. Immunol. Methods* **1988**, *112*, 113–120.
- (5) Kausaite-Minkstiniene, A.; Ramanaviciene, A.; Kirlyte, J.; Ramanavicius, A. Comparative study of random and oriented antibody immobilization techniques on the binding capacity of immunosensor. *Anal. Chem.* **2010**, *82*, 6401–6408.
- (6) Silvertown, E. W.; Navia, M. A.; Davies, D. R. Three-dimensional structure of an intact human immunoglobulin. *Proc. Natl. Acad. Sci. U. S. A.* **1977**, *74*, 5140–5144.
- (7) Moyle, W. R.; Lin, C.; Corson, R. L.; Ehrlich, P. H. Quantitative explanation for increased affinity shown by mixtures of monoclonal antibodies: importance of a circular complex. *Mol. Immunol.* **1983**, *20*, 439–452.
- (8) Spitznagel, T. M.; Clark, D. S. Surface-density and orientation effects on immobilized antibodies and antibody fragments. *Nat. Biotechnol.* **1993**, *11*, 825–829.
- (9) Yoshimoto, K.; Nishio, M.; Sugawara, H.; Nagasaki, Y. Direct observation of adsorption-induced inactivation of antibody fragments surrounded by mixed-PEG layer on a gold surface. *J. Am. Chem. Soc.* **2010**, *132*, 7982–89.
- (10) Xu, H.; Zhao, X.; Grant, C.; Lu, J. R.; Williams, D. E.; Penfold, J. Orientation of a monoclonal antibody adsorbed at the solid/solution interface: a combined study using atomic force microscopy and neutron reflectivity. *Langmuir* **2006**, *22*, 6313–6320.
- (11) Penfold, J.; Richardson, R. M.; Zorbakhsh, A.; Webster, J. R.; Bucknall, D. G.; Rennie, A. R.; Jones, R. A.; Cosgrove, T.; Thomas, R. K.; Higgins, J. S.; Fletcher, P. D.; Dickinson, E.; Roser, S. J.; McLure, I. A.; Hillman, A. R.; Richards, R. W.; Staples, E. J.; Burgess, A. N.; Simister, E. A.; White, J. W. Recent advances in the study of chemical surfaces and interfaces by specular neutron reflection. *J. Chem. Soc., Faraday Trans.* **1997**, *93*, 3899–3917.
- (12) Fragneto, G.; Thomas, R. K.; Rennie, A. R.; Penfold, J. Neutron reflection study of bovine beta-casein adsorbed on OTS self-assembled monolayers. *Science* **1995**, *267*, 657–660.
- (13) Penfold, J.; Thomas, R. K. The application of the specular reflection of neutrons to the study of surfaces and interfaces. *J. Phys.: Condens. Matter* **1990**, *2*, 1369–1412.
- (14) Hayter, J. B.; Highfield, R. R.; Pullman, B. J.; Thomas, R. K.; McMullen, A. I.; Penfold, J. Critical reflection of neutrons. A new technique for investigating interfacial phenomena. *J. Chem. Soc., Faraday Trans. 1* **1981**, *77*, 1437–1448.
- (15) Born, M.; Wolf, E. *Principles of Optics*; Pergamon: Oxford, 1970.
- (16) Latter, E. Protein adsorption at the solid/liquid interface: a neutron reflectivity study, D. Phil. Thesis, University of Oxford, 2012.
- (17) Glatz, J. F.; Veerkamp, J. H. Removal of fatty acids from serum albumin by Lipidex 1000 chromatography. *J. Biochem. Biophys. Methods* **1983**, *8*, 57–61.
- (18) Liebmman Vinson, A.; Lander, L. M.; Foster, M. D.; Brittain, W. J.; Vogler, E. A.; Majkrzak, C. F.; Satija, S. A neutron reflectometry study of human serum albumin adsorption in situ. *Langmuir* **1996**, *12*, 2256–62.
- (19) Olivier, J. R.; Craievich, A. F. The subdomain structure of human serum albumin in solution under different pH conditions studied by small angle X-ray scattering. *Eur. Biophys. J.* **1995**, *24*, 77–84.
- (20) Sugio, S.; Kashima, A.; Mochizuki, S.; Noda, M.; Kobayashi, K. Crystal structure of human serum albumin at 2.5 Å resolution. *Protein Eng.* **1999**, *12*, 439–446.
- (21) Kosmulski, M. *Chemical Properties of Material Surfaces*; Dekker: New York, 2001.
- (22) Choi, E. J.; Foster, M. D.; Daly, S.; Tilton, R.; Przybycien, T.; Majkrzak, C. F.; Witte, P.; Menzel, H. Effect of flow on human serum albumin adsorption to self-assembled monolayers of varying packing density. *Langmuir* **2003**, *19*, 5464–74.
- (23) Cowsill, B. J.; Coffey, P. D.; Yaseen, M.; Waigh, T. A.; Freeman, N. J.; Lu, J. R. Measurement of the thickness of ultra-thin adsorbed globular protein layers with dual-polarisation interferometry: a comparison with neutron reflectivity. *Soft Matter* **2011**, *7*, 7223–7230.
- (24) Zhao, X.; Pan, F.; Cowsill, B. J.; Lu, J. R.; Garcia-Gancedo, L.; Flewitt, A. J.; Ashley, G. M.; Luo, J. Interfacial immobilization of monoclonal antibody and detection of human prostate-specific antigen. *Langmuir* **2011**, *27*, 7654–7662.
- (25) Cowsill, B. J.; Waigh, T. A.; Eapen, S.; Davies, R.; Lu, J. R. Interfacial structure and history dependent activity of immobilised antibodies in model pregnancy tests. *Soft Matter* **2012**, *8*, 9847–9854.